Dynamics of noise-like pulsing at sub-ns scale in a passively mode-locked fiber laser

H. Santiago-Hernandez,[1,*] O. Pottiez,[1] M. Duran-Sanchez,[2,3] R. I. Alvarez-Tamayo,[2] J. P. Lauterio-Cruz,[1] J. C. Hernandez-Garcia,[4] B. Ibarra-Escamilla,[2] and E. A. Kuzin[2]

[1] *Centro de Investigaciones en Óptica (CIO), Loma del Bosque 115, Col. Lomas del Campestre, León, Gto. 37150, Mexico*

[2] *Instituto Nacional de Astrofísica, Óptica y Electrónica (INAOE), L. E. Erro 1, Sta. Ma. Tonantzintla, Pue. 72824, Mexico*

[3] *Consejo Nacional de Ciencia y Tecnología (CONACyT), Av. Insurgentes Sur No. 1582, Col. Crédito Constructor, Del. Benito Juárez, C. P. 039040, México D. F., Mexico*

[4] *Departamento de Electrónica, División de Ingenierías Campus Irapuato-Salamanca, Universidad de Guanajuato, Carretera Salamanca-Valle de Santiago Km 3.5 + 1.8 Km, Comunidad de Palo Blanco, Salamanca, Gto. 36885, Mexico*

**fis_hsh@cio.mx*

Abstract: We report an original noise-like pulse dynamics observed in a figure-eight fiber laser, in which fragments are continually released from a main waveform that circulates in the cavity. Particularly, we report two representative cases of the dynamics: in the first case the released fragments drift away from the main bunch and decay over a fraction of the round-trip time, and then vanish suddenly; in the second case, the sub-packets drift without decaying over the complete cavity round-trip time, until they eventually merge again with the main waveform. The most intriguing result is that these fragments, as well as the main waveform, are formed of units with sub-ns duration and roughly the same energy.

OCIS codes: (140.3510) Lasers, fiber; (140.4050) Mode-locked lasers; (060.5530) Pulse propagation and temporal solitons.

References and links

1. H. A. Haus, "Theory of mode locking with a fast saturable absorber," Appl. Phys. (Berl.) **46**(7), 3049–3058 (1975).
2. F. Krausz, T. Brabec, and C. Spielmann, "Self-starting passive mode locking," Opt. Lett. **16**(4), 235–237 (1991).
3. V. J. Matsas, D. J. Richardson, T. P. Newson, and D. N. Payne, "Characterization of a self-starting, passively mode-locked fiber ring laser that exploits nonlinear polarization evolution," Opt. Lett. **18**(5), 358–360 (1993).
4. H. A. Haus, E. P. Ippen, and K. Tamura, "Additive-pulse modelocking in fiber lasers," IEEE J. Quantum Electron. **30**(1), 200–208 (1994).
5. L. E. Nelson, D. J. Jones, K. Tamura, H. A. Haus, and E. P. Ippen, "Ultrashort-pulse fiber ring lasers," Appl. Phys. B **65**(2), 277–294 (1997).
6. K. Tamura, E. P. Ippen, H. A. Haus, and L. E. Nelson, "77-fs pulse generation from a stretched-pulse mode-locked all-fiber ring laser," Opt. Lett. **18**(13), 1080–1082 (1993).
7. F. Ö. Ilday, J. R. Buckley, W. G. Clark, and F. W. Wise, "Self-similar evolution of parabolic pulses in a laser," Phys. Rev. Lett. **92**(21), 213902 (2004).
8. A. Chong, J. Buckley, W. Renninger, and F. Wise, "All-normal-dispersion femtosecond fiber laser," Opt. Express **14**(21), 10095–10100 (2006).
9. L. M. Zhao, D. Y. Tang, X. Wu, and H. Zhang, "Dissipative soliton trapping in normal dispersion-fiber lasers," Opt. Lett. **35**(11), 1902–1904 (2010).
10. N. Akhmediev, J. M. Soto-Crespo, and P. Grelu, "Roadmap to ultra-short record high-energy pulses out of laser oscillators," Phys. Lett. A **372**(17), 3124–3128 (2008).
11. H. Lin, C. Guo, S. Ruan, and J. Yang, "Dissipative soliton resonance in an all-normal-dispersion Yb-doped figure-eight fibre laser with tunable output," Laser Phys. Lett. **11**(8), 085102 (2014).
12. A. B. Grudinin, D. J. Richardson, and D. N. Payne, "Energy quantisation in figure eight fibre laser," Electron. Lett. **28**(1), 67–68 (1992).
13. A. B. Grudinin and S. Gray, "Passive harmonic mode locking in soliton fiber lasers," J. Opt. Soc. Am. B **14**(1), 144–154 (1997).

#242371 Received 4 Jun 2015; revised 6 Jul 2015; accepted 7 Jul 2015; published 13 Jul 2015

14. D. Y. Tang, B. Zhao, L. M. Zhao, and H. Y. Tam, "Soliton interaction in a fiber ring laser," Phys. Rev. E Stat. Nonlin. Soft Matter Phys. **72**(1), 016616 (2005).
15. F. Amrani, A. Haboucha, M. Salhi, H. Leblond, A. Komarov, and F. Sanchez, "Dissipative solitons compounds in a fiber laser. Analogy with the states of the matter," Appl. Phys. B **99**(1–2), 107–114 (2010).
16. M. Horowitz and Y. Silberberg, "Control of noiselike pulse generation in erbium-doped fiber lasers," IEEE Photonics Technol. Lett. **10**(10), 1389–1391 (1998).
17. D. Tang, L. Zhao, and B. Zhao, "Soliton collapse and bunched noise-like pulse generation in a passively mode-locked fiber ring laser," Opt. Express **13**(7), 2289–2294 (2005).
18. L. M. Zhao and D. Y. Tang, "Generation of 15-nJ bunched noise-like pulses with 93-nm bandwidth in an erbium-doped fiber ring laser," Appl. Phys. B **83**(4), 553–557 (2006).
19. L. M. Zhao, D. Y. Tang, J. Wu, X. Q. Fu, and S. C. Wen, "Noise-like pulse in a gain-guided soliton fiber laser," Opt. Express **15**(5), 2145–2150 (2007).
20. S. Kobtsev, S. Kukarin, S. Smirnov, S. Turitsyn, and A. Latkin, "Generation of double-scale femto/pico-second optical lumps in mode-locked fiber lasers," Opt. Express **17**(23), 20707–20713 (2009).
21. L. A. Vazquez-Zuniga and Y. Jeong, "Super-broadband noise-like pulse erbium-doped fiber ring laser with a highly nonlinear fiber for Raman gain enhancement," IEEE Photonics Technol. Lett. **24**(17), 1549–1551 (2012).
22. A. Boucon, B. Barviau, J. Fatome, C. Finot, T. Sylvestre, M. W. Lee, P. Grelu, and G. Millot, "Noise-like pulses generated at high harmonics in a partially-mode-locked km-long Raman fiber laser," Appl. Phys. B **106**(2), 283–287 (2012).
23. X. He, A. Luo, Q. Yang, T. Yang, X. Yuan, S. Xu, Q. Qian, D. Chen, Z. Luo, W. Xu, and Z. Yang, "60nm bandwidth, 17 nJ noiselike pulse generation from a thulium-doped fiber ring laser," Appl. Phys. Express **6**(11), 112702 (2013).
24. A. K. Zaytsev, C. H. Lin, Y. J. You, F. H. Tsai, C. L. Wang, and C. L. Pan, "A controllable noise-like operation regime in a Yb-doped dispersion-mapped fiber ring laser," Laser Phys. Lett. **10**(4), 045104 (2013).
25. T. North and M. Rochette, "Raman-induced noiselike pulses in a highly nonlinear and dispersive all-fiber ring laser," Opt. Lett. **38**(6), 890–892 (2013).
26. O. Pottiez, B. Ibarra-Escamilla, E. A. Kuzin, J. C. Hernández-García, A. González-García, and M. Durán-Sánchez, "Multiple noise-like pulsing of a figure-eight fibre laser," Laser Phys. **24**(1), 015103 (2014).
27. O. Pottiez, J. C. Hernández-García, B. Ibarra-Escamilla, E. A. Kuzin, M. Durán-Sánchez, and A. González-García, "High-order harmonic noise-like pulsing of a passively mode-locked double-clad Er/Yb fibre ring laser," Laser Phys. **24**(11), 115103 (2014).
28. Y. Jeong, L. A. Vazquez-Zuniga, S. Lee, and Y. Kwon, "On the formation of noise-like pulses in fiber ring cavity configurations," Opt. Fiber Technol. **20**(6), 575–592 (2014).
29. Y. S. Fedotov, A. V. Ivanenko, S. M. Kobtsev, and S. V. Smirnov, "High average power mode-locked figure-eight Yb fibre master oscillator," Opt. Express **22**(25), 31379–31386 (2014).
30. D. V. Churkin, S. Sugavanam, N. Tarasov, S. Khorev, S. V. Smirnov, S. M. Kobtsev, and S. K. Turitsyn, "Stochasticity, periodicity and localized light structures in partially mode-locked fibre lasers," Nat. Commun. **6**, 7004 (2015).
31. W. Chang, J. M. Soto-Crespo, P. Vouzas, and N. Akhmediev, "Spiny solitons and noise-like pulses," J. Opt. Soc. Am. B **32**(7), 1377–1383 (2015).
32. A. Zaytsev, C. H. Lin, Y. J. You, C. C. Chung, C. L. Wang, and C. L. Pan, "Supercontinuum generation by noise-like pulses transmitted through normally dispersive standard single-mode fibers," Opt. Express **21**(13), 16056–16062 (2013).
33. S. V. Smirnov, S. M. Kobtsev, and S. V. Kukarin, "Efficiency of non-linear frequency conversion of double-scale pico-femtosecond pulses of passively mode-locked fiber laser," Opt. Express **22**(1), 1058–1064 (2014).
34. S. Kobtsev, S. Kukarin, S. Smirnov, and I. Ankudinov, "Cascaded SRS of single- and double-scale fiber laser pulses in long extra-cavity fiber," Opt. Express **22**(17), 20770–20775 (2014).
35. V. Goloborodko, S. Keren, A. Rosenthal, B. Levit, and M. Horowitz, "Measuring temperature profiles in high-power optical fiber components," Appl. Opt. **42**(13), 2284–2288 (2003).
36. K. Özgören, B. Öktem, S. Yilmaz, F. Ö. Ilday, and K. Eken, "83 W, 3.1 MHz, square-shaped, 1 ns-pulsed all-fiber-integrated laser for micromachining," Opt. Express **19**(18), 17647–17652 (2011).
37. H. L. Yu, P. F. Ma, R. M. Tao, X. L. Wang, P. Zhou, and J. B. Chen, "High average/peak power linearly polarized all-fiber picosecond MOPA seeded by mode-locked noise-like pulses," Laser Phys. Lett. **12**(6), 065103 (2015).
38. C. Lecaplain and P. Grelu, "Rogue waves among noiselike-pulse laser emission: an experimental investigation," Phys. Rev. A **90**(1), 013805 (2014).
39. A. F. J. Runge, C. Aguergaray, N. G. R. Broderick, and M. Erkintalo, "Raman rogue waves in a partially mode-locked fiber laser," Opt. Lett. **39**(2), 319–322 (2014).
40. H. Santiago-Hernandez, O. Pottiez, R. Paez-Aguirre, H. E. Ibarra-Villalon, A. Tenorio-Torres, M. Duran-Sanchez, B. Ibarra-Escamilla, E. A. Kuzin, and J. C. Hernandez-Garcia, "Generation and characterization of erbium-Raman noise-like pulses from a figure-eight fibre laser," Laser Phys. **25**(4), 045106 (2015).
41. E. A. Kuzin, N. Korneev, J. W. Haus, and B. Ibarra-Escamilla, "Theory of nonlinear loop mirrors with twisted low-birefringence fiber," J. Opt. Soc. Am. B **18**(7), 919–925 (2001).
42. C. Lecaplain, P. Grelu, J. M. Soto-Crespo, and N. Akhmediev, "Dissipative rogue wave generation in multiple-pulsing mode-locked fiber laser," J. Opt. **15**(6), 064005 (2013).

#242371 Received 4 Jun 2015; revised 6 Jul 2015; accepted 7 Jul 2015; published 13 Jul 2015

43. F. Sanchez, Ph. Grelu, H. Leblond, A. Komarov, K. Komarov, M. Salhi, A. Niang, F. Amrani, C. Lecaplain, and S. Chouli, "Manipulating dissipative soliton ensembles in passively mode-locked fiber lasers," Opt. Fiber Technol. **20**(6), 562–574 (2014).
44. S. Chouli and P. Grelu, "Soliton rains in a fiber laser: an experimental study," Phys. Rev. A **81**(6), 063829 (2010).
45. S. Chouli and P. Grelu, "Rains of solitons in a fiber laser," Opt. Express **17**(14), 11776–11781 (2009).

1. Introduction

More than 20 years have elapsed since the fundamental knowledge about passive mode locking was established [1–4]. As high power pump diodes have become readily available, there has been a special interest in the passively mode-locked fiber lasers technology for the generation of stable ultra-short pulses, including the net anomalous dispersion regime that generates conventional soliton pulses [5], the dispersion-managed soliton regime [6], the self-similar pulse regime [7], the all normal dispersion (ANDi) regime [8,9], and the dissipative soliton resonance regime [10,11]. Even further, in the anomalous dispersion regime, as pump power is increased, multiple solitons tend to appear in the cavity, all sharing the same properties (soliton quantization) [12]. Multiple soliton regimes have been extensively observed where several tens or hundreds of pulses coexist and interact in the cavity in various ways [13,14], resulting in the emergence of a wide variety of "states" [15]. Moreover, it has been reported that the passively mode-locked fiber lasers can switch to a radically different mode of operation, the so called "Noise-like pulse" (NLP) regime [16–31], which is the regime under study in the present work.

The NLP regime is typical of relatively long and/or highly pumped fiber laser cavities, and is quite universal, as it has been observed for a wide span of laser architectures, dispersion regimes or operating wavelengths. Its study is attractive on the fundamental level, due to its extremely rich dynamics which is barely starting to be unveiled [30,31], and whose understanding remains highly challenging. Getting a clear picture of such complex non-stationary regimes would have far-reaching implications, in particular it would help understand and push back the limits of more standard, stationary regimes [5–11]. Besides, considering their properties such as a high energy, wide optical bandwidth and short coherence time, NLPs are attractive for several important applications including supercontinuum generation [32], nonlinear frequency conversion [33,34], sensing [35] or micromachining [36], among others. Average powers up to the watt range directly at the laser output are readily achievable [29]. Using an all-fiber master oscillator power amplifier (MOPA) configuration, NLP energies of a few tens of micro-joules and peak powers up to one third of a megawatt have been achieved recently [37], which further illustrates the potential of such sources for the above-mentioned applications. In the field of fundamental physics, these complex pulses also constitute an ideal platform for the study of optical rogue waves [38,39]. Both experimental and numerical studies suggest that noise-like pulses are long (ps-ns) and compact wave packets composed of a very large number of ultra-short (~100 fs) internal sub-pulses with random amplitudes and durations that vary quickly in a complicated manner. In addition to the double fs/ns time scale, an intermediary level of organization was discovered recently at the sub-ns scale [40], which further increases the internal complexity of these objects. Despite the complexity and variability of their fine structure, generally the NLPs display a very simple and stable overall behavior. In particular, a stable, wide and smooth, structureless optical spectrum and a double-scaled autocorrelation, with a narrow coherence peak riding a wide pedestal are the identifying signatures of this regime. In addition, the energy of the bunch and its total duration are also relatively stable for given cavity settings. Moreover, typically a single NLP is observed in the cavity, even though a few works have reported multiple noise-like pulsing [16,26], or even harmonic mode locking [22,27]. Unlike multiple soliton regimes, for which a wide spectrum of collective behaviors can be explored experimentally using fast optoelectronics [15], the subtle dynamics of NLPs taking place at the sub-ps scale remains orders of magnitude beyond the reach of

#242371 Received 4 Jun 2015; revised 6 Jul 2015; accepted 7 Jul 2015; published 13 Jul 2015

even the fastest detection schemes, and can only be explored numerically [17–20,26,28]. In contrast, at longer time scales ranging from tens to hundreds of ps, which are still well below the duration of typical NLPs but are much more accessible experimentally, no relevant dynamical behavior is usually found (one notable exception however can be found in [30]).

In this work, we report what we believe is the first experimental demonstration of a peculiar dynamics observed at sub-ns scale in a passively mode-locked fiber laser in NLP operation, in which sub-units from a main bunch are continually released. The evolution of the drifting sub-pulses can be modified by slight adjustments of wave retarders. In some cases they drift and decay until they eventually vanish after a fraction of the round-trip time, whereas in other cases they maintain themselves over the whole period until they merge again with the main NLP, thus filling completely the cavity.

2. Experimental setup and results

Experiments are performed with the laser setup shown schematically in Fig. 1. The figure-eight laser is formed by a NOLM inserted in a ring laser cavity. The total cavity length is ~225 m. The output ports are provided by two 90/10 couplers. The ring cavity includes an optical isolator that ensures unidirectional laser operation. A section of dispersion compensating fiber (DCF) of 100 m with D = –3ps/nm/km is inserted in the ring section. The ring also includes two sections of erbium-doped fiber (EDF) with 30-dB m^{-1} absorption at 1530 nm: 3-m EDF1 and 2-m EDF2. The EDFs are pumped at 980 nm through WDM couplers. The pump powers into EDF1 and EDF2 are ~300 mW and ~200 mW, respectively. The cavity contains a polarizer and a polarization controller (PC) consisting of two retarder plates of λ/2 (HWR1) and λ/4 (QWR1), respectively. The PC is used to maximize the power transmission through the polarizer. The nonlinear optical loop mirror (NOLM) is a power-symmetric, polarization-imbalanced scheme, whose switching relies on nonlinear polarization evolution in the twisted loop [41]. It is made of a 50/50 coupler, 100 m of Corning SMF-28, low-birefringence fiber (D = 17 ps/nm/km) twisted at a rate of 5 turns/m, and a quarter-wave retarder (QWR2). To control the angle of linear polarization at the NOLM input, a half-wave retarder (HWR2) is implemented. The net cavity dispersion is estimated to be + 2.08ps/nm. As the ring section of the laser is large, is made of non-polarization-maintaining fiber and includes a polarizer, it is possible that the mode locking mechanism involves both the NOLM and nonlinear polarization evolution in the ring section [3].

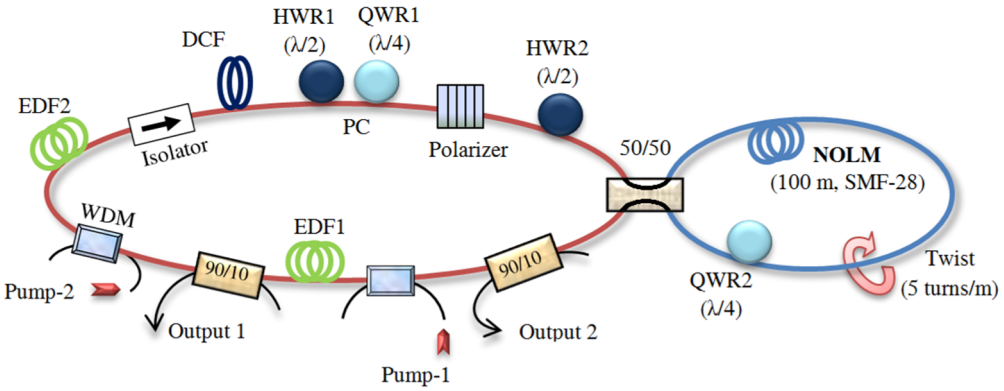

Fig. 1. Scheme of the figure-eight fiber laser.

For some positions of the PC, when a mechanical stimulation is applied, we obtain a stable mode locking operation. In this regime, the average output power (measured at output 1) is ~9-10 mW. On the scope, as shown in Fig. 2(a), mode locking is evidenced by the appearance of a stable train of pulses with a period of T = 1.12 μs, meaning that a single pulse

#242371 Received 4 Jun 2015; revised 6 Jul 2015; accepted 7 Jul 2015; published 13 Jul 2015

circulates in the 225-m long cavity (fundamental mode locking). The pulse is also measured in the time domain using a 25-GHz photodetector and a 50-GHz sampling scope, as shown in Fig. 2(b); the measurement shows that the average pulse envelope has a squared waveform and a duration of ~4ns. The optical spectrum of fundamental mode locking is depicted in Fig. 2(c). A wide and smooth spectrum is obtained, with a maximum near 1560 nm. The 3-dB bandwidth is 13 nm. The portion of the spectrum around 1650 nm corresponds to the Raman scattering effect. The autocorrelation trace is shown in Fig. 2(d) presenting a narrow (~500-fs) peak riding a wide pedestal that extends beyond the 200-ps measurement window of the autocorrelator. These features confirm the noise-like nature of the generated pulses.

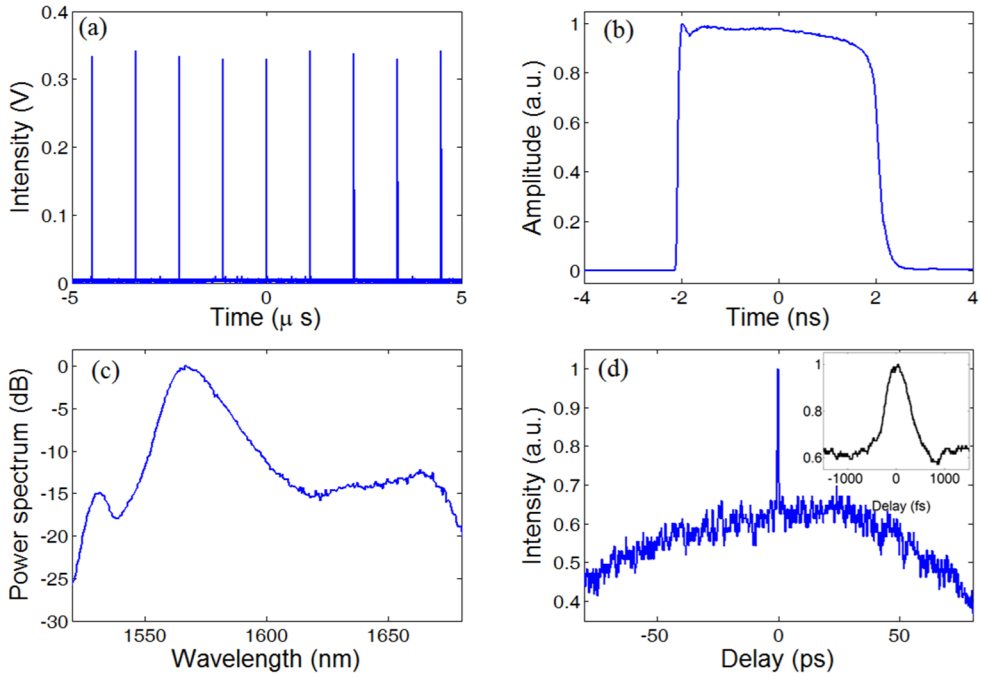

Fig. 2. Fundamental mode locking: (a) Oscilloscope trace of pulse train obtained using a 2-GHz photodetector and a 200-MHz oscilloscope, (b) time-domain envelope measured using a 25-GHz photodetector and a 50-GHz sampling scope, (c) Optical spectra observed at output-2, (d) autocorrelation trace (inset shows a close-up on the central spur).

Once that mode locking is achieved, the release of sub-pulses by the NLP is observed by making small adjustments of HWR2, as shown in Fig. 3; several sub-packets of NLPs emerge randomly from the main packet and drift and decay slightly in both directions (although mostly to the right), until they suddenly disappear after some fraction of the cavity period, when their amplitude is still far from zero (HWR2 positions 1-2 in Fig. 3; see also Visualization 1). If the HWR2 is further adjusted, the released sub-pulses are able to drift farther before vanishing but, in this case, only to the right side of the main pulse, as shown in Fig. 3 at HWR2 positions 3 and 4. If the HWR2 adjustment continues, the released sub-pulses drift still farther, until they no longer decay and, after drifting over the whole period, they are finally recaptured by the main NLP. In this case the multiple pulses completely fill the cavity, and coexist with the main pulse in a disordered way, just as shown at position-5 in Fig. 3 (see Visualization 2). The sub-pulses observed to the left side at position-5 are those that were previously released from the main packet and are reaching it again after drifting over one complete round-trip. In all cases described above, sub-pulses are continuously released (and in the last case, recaptured) by the main NLP, and the process goes on indefinitely in a quasi-stationary fashion. The optical spectra and autocorrelation traces corresponding to the sub-

#242371 Received 4 Jun 2015; revised 6 Jul 2015; accepted 7 Jul 2015; published 13 Jul 2015

pulse release regime are very similar to those of stable fundamental mode locking shown in Figs. 2(c) and 2(d), respectively, with a 20-50% increase in the bandwidth of the optical spectra. This confirms that these complex behaviours still belong globally to the noise-like pulsing mode of operation of the laser.

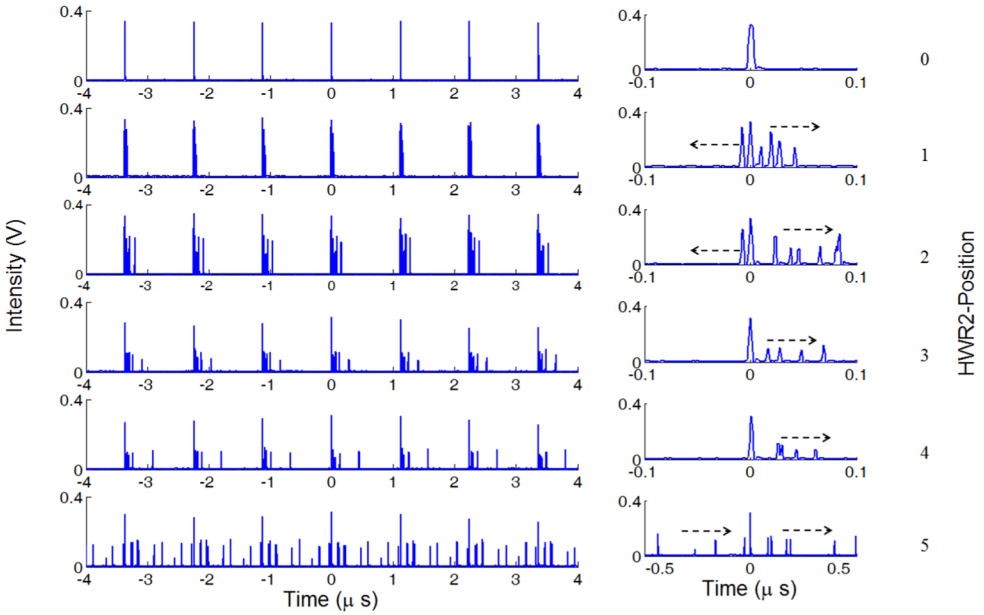

Fig. 3. Evolution of the NLP dynamics observed with a 2-GHz photodetector and 200-MHz oscilloscope in single-shot mode, as the position of HWR2 is varied: the left figures display ~7 cavity periods, and the right figures present a close-up on the central portion of each trace. The arrows indicate the direction of propagation of the sub-pulses released by the central waveform. See also Visualization 1 and Visualization 2.

We analyzed statistically the energy of the pulses released from the main waveform through the construction of histograms. Sixty measurements were performed with a 2-GHz photodetector and 200-MHz oscilloscope in single-shot acquisition mode. Due to the limited bandwidth of the detection setup, the peak amplitudes measured on the scope were directly proportional to the energy of the pulses. The energy distributions were obtained by combining the data of sixty single-shot measurements. In each measurement, the energies attained by the main pulse and all the released sub-pulses appearing between -T/2 and + T/2 were captured (dots in Fig. 4). The energy histograms are shown in two representative cases: when the sub-pulses are released, drift and decay until they eventually disappear, in Fig. 4(a); and when the sub-pulses drift throughout the cavity before merging with the main packet, in Fig. 4(b). In Fig. 4(a), the concentration of red dots on both sides of the main waveform (blue dots) indicates that sub-pulses drift in both directions, although the number of dots on the right side is by far superior. The trend of the sub-pulses to decay as they move away from the main packet is also visible in this figure. Finally, the abrupt disappearance of the dots at roughly one fifth of the cavity round-trip time in each direction indicates that the sub-pulses vanish beyond some distance from the original waveform. In contrast, the red dots in Fig. 4(b) are uniformly scattered over the entire period, showing no evidence of amplitude decay as the distance from the main pulse (blue dots) increases. In each case, the histograms reveal that the sub-pulses are more likely to present certain energy levels, as shown in Figs. 4(a) and 4(b); both cases show evidence that the values of energy concentrate around three discrete levels: 0.13 V, 0.24 V, and 0.31 V; the highest level corresponds to the main pulse (t = 0), and the other two correspond to the released packets. The relative amplitudes of the histograms at

#242371 Received 4 Jun 2015; revised 6 Jul 2015; accepted 7 Jul 2015; published 13 Jul 2015

0.13 V and 0.24 V also reveal that the first level is significantly more frequent than the second. In both cases, the energies of the released bunches are roughly in a ratio of one to two. Besides, the clear-cut division between the histogram peaks at 0.13 V and 0.24 V in Fig. 4(b) is quite remarkable: almost no sub-pulse energy is found in the vicinity of 0.18 V (see the clear interval between the two bands of scattered dots in this figure). In Fig. 4(a), the decay of the sub-pulses as they move away from the main packet contributes to blur slightly the separation between the two peaks. Finally, Figs. 4(c) and 4(d) show the variations in the energy of the main waveform across the sixty measurements depicted in Figs. 4(a) and 4(b), respectively. The fitting line shown in Figs. 4(c) and 4(d) reveals that the energy of the main waveform remains almost constant (~0.32 V) for both cases.

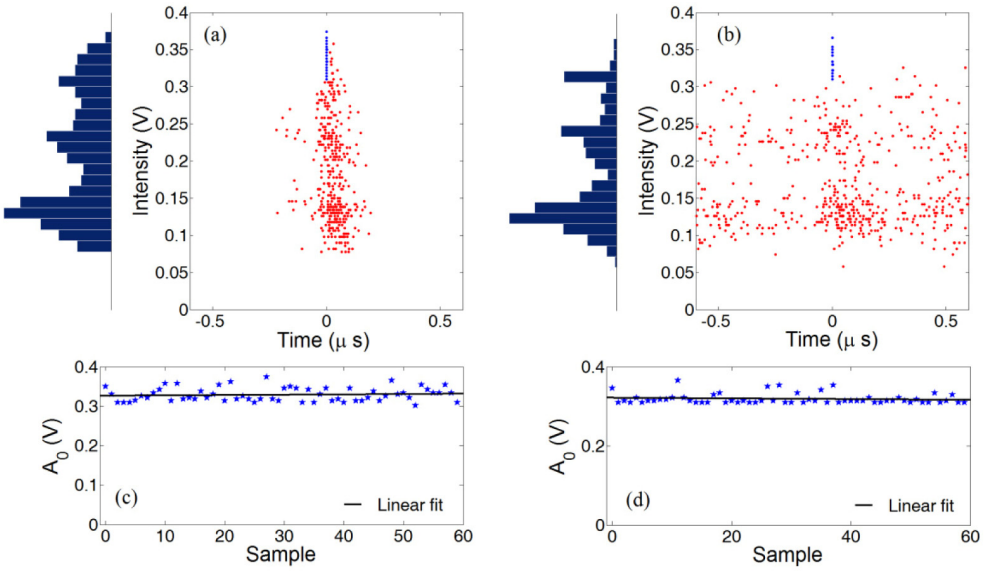

Fig. 4. Statistical analysis of the energies of the sub-pulses (a) when the drifting sub-pulses decay and finally disappear and (b) when the sub-pulses drift throughout the cavity; (c) and (d) Energy of main pulse extracted from data in (a) and (b), respectively.

The temporal profiles obtained using a 25-GHz photodetector and 50-GHz sampling scope are displayed in Fig. 5, for the two cases already presented in Fig. 4. These curves span over a short time interval of a few tens of ns, covering the main packet and its close vicinity. The temporal profiles resulting of averaging 1024 samples (Curves 0) displayed in Figs. 5(a) and 5(b) both show an intense and narrow pulse followed by a long, low-intensity tail. The traces obtained without averaging (curves 1 to 8) depicted in Figs. 5(a) and 5(b) are taken in the same conditions but at different times; these traces are more illustrative of the dynamics of the wave packet. Although a sampling scope does not allow single-shot measurements, the duration of each measurement is sufficiently short (a fraction of a millisecond, corresponding to a few hundreds of round-trips) so that we can assume that the waveform envelope suffers no drastic changes at nanosecond scale during that time; in order to support this hypothesis, we recorded up to 100 consecutive periods of the laser emission using the 200-MHz oscilloscope, observing no noticeable variation of the waveform (in particular, in the position of the drifting sub-pulses) over this sequence of 100 cycles. Moreover, considering that with the sampling scope, the measurement is triggered by the signal itself, the slow variation of the waveform even at the scale of hundreds of round-trip times ensured consistent triggering during the measurement of each trace. When the trigger level was sufficiently high, triggering was performed on the rising edge of the main waveform, so that its position is maintained in all traces of Fig. 5. Curves without averaging in Fig. 5 show that the main pulse is actually

#242371 Received 4 Jun 2015; revised 6 Jul 2015; accepted 7 Jul 2015; published 13 Jul 2015

formed of a collection of roughly identical sub-units with a sub-ns duration, whose number and separation vary widely between the measurements. The relative displacements between these sub-units explain the profile obtained in the averaged measurements, in particular the long tail. It has to be noted that a NLP substructure of jittering sub-ns units is probably present even in the stable mode locking regime, as attested by the sub-ns duration of the pedestal of autocorrelation in Fig. 2(d), much shorter than the 4-ns NLP duration observed in Fig. 2(b) (the presence of a small spike on the left edge of this envelope is another indication of the existence of these sub-units; the rest of the envelope is gently sloping due to timing jitter affecting sub-units and strong averaging). The same curves without averaging in Figs. 5(a) and 5(b) show a few sub-units that separate from the main bunch and are starting to drift away on the right side of the main packet (in Fig. 5(b), curves 1 and 5 also show sub-units on the left side drifting back to the main bunch). Although most of them appear as individual units, some appear to be associated in pairs (although direct measurements using a fast real-time oscilloscope were not performed, we believe that the data of Fig. 5 are indicative of the existence of such pairs of sub-units). Finally, Figs. 5(c) and 5(d) show the energy of the main packet obtained by integration of the data of Figs. 5(a) and 5(b), respectively. These figures show strong energy variations, which contrast with Figs. 4(c) and 4(d).

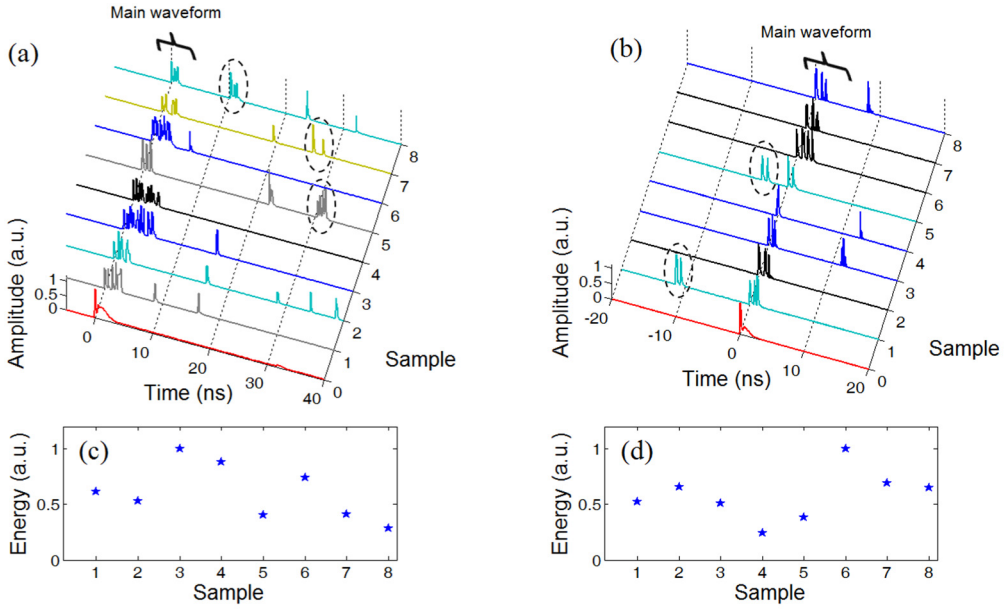

Fig. 5. Temporal profiles of two representative cases of noise-like pulse dynamics, obtained using a 25-GHZ photodetector and 50-GHz sampling scope: (a) the sub-units drift and decay over a short time, and (b) the sub-units drift over the whole cavity, (c) and (d) energy of the main pulse obtained by integration of the main waveform using data 1 to 8 in (a) and (b), respectively. Sample-0 acquired with average = 1024, and curves 1 to 8 without averaging. Drifting pairs are indicated by dashed circles.

3. Discussion

In a recent work by the authors [40], the NLPs produced in a fiber laser scheme similar to the one studied here have revealed an intermediate level of organization in their temporal waveform, at the sub-ns scale, forming sub-structures that include a large number of femtosecond sub-pulses (the ultimate unit in noise-like pulses, revealed by the coherence spike of autocorrelation) but significantly smaller than the full NLP. In the present work, similar intermediate units, with a duration of ~0.1 ns and roughly the same energy, appear in the constitution of the main waveform in Figs. 5(a) and 5(b), and it is also clear from the same

#242371 Received 4 Jun 2015; revised 6 Jul 2015; accepted 7 Jul 2015; published 13 Jul 2015

figures that they are the elements that at some point get loose from the main packet and start drifting away from it. Although most of these units appear to drift alone, some of them are grouped by two. Considering that these units have approximately the same energy, it becomes clear that the existence of two discrete energy levels of drifting waveforms observed in Fig. 4 and the ratio of 1:2 between them is directly connected to the existence of these units traveling alone or in pairs. Besides, the larger amplitude of the histograms at the lower discrete level as compared to the higher level in Fig. 4 is also consistent with the larger number of individual units observed in Fig. 5, in comparison with pairs.

The apparent discrepancies between Figs. 4(c) and 4(d) and Figs. 5(c) and 5(d) concerning the variation of the main bunch energy are a clear illustration of how the detection bandwidth affects the result of a measurement (e.g., see [42]). Figure 5 (obtained with 25-GHz resolution) shows that, just after releasing one or several units, logically the number of units remaining in the main packet and, therefore, the energy of the remaining packet, are small. Shortly after that, however, new units emerge, presumably from the background radiation, so that the energy of the main bunch can be restored, a necessary condition for a quasi-stationary evolution to be maintained. In the case of Fig. 5(b), the recapture of sub-units arriving on the left also contributes to the recovery of the main bunch. This dynamics, which is associated with large fluctuations of the energy of the main packet, can be compared to the soliton rain/release of solitons dynamics, where the energy of the "condensed phase" and its number of solitons is subjected to similar variations [43]. In contrast, in the 200-MHz, low-resolution measurement (Fig. 4), the recently released drifting units at first are close to the main bunch and cannot be distinguished from it, and by the time they are distinguishable, other units have been recaptured or new internal units have already emerged in the main waveform, ensuring that only marginal variations of its energy are registered.

As already mentioned, the NLP dynamics reported here bears some analogy with the rain of solitons/soliton release dynamics [43–45]. It makes sense since both types of phenomena are obvious manifestations of dissipative nonlinear dynamics. Besides, both regimes are observed in the anomalous regime of dispersion and rely profoundly on polarization adjustments and nonlinear polarization evolution. In the present case however, the solitons are replaced by sub-ns units with sub-ps coherence which, for some reasons that still have to be clarified, present roughly the same energy. It has to be stressed also that only a dynamics of release has been observed, as no equivalent of the "rain" dynamics (units emerging from the background radiation and drifting towards the bunch) has been evidenced. Like in the case of multiple soliton regimes, dissipative nonlinear effects would be of key relevance to analyze the puzzling temporal evolution reported here, with a main pulse that manages to maintain itself in spite of large energy variations, and drifting units that either decay and vanish abruptly, or travel over a full period. Finally, like in the case of multiple solitons dynamics [13,14,43], it is likely that background radiation components mediate some kind of interaction between the units of the NLP, weakening its cohesion and causing the drift. Such interactions could also be invoked to understand the formation of drifting pairs. Although no continuous-wave component is observed in the spectrum of Fig. 2(c), it includes a peak at 1530 nm, which was shown to originate from amplified spontaneous emission [40], and a Raman component around 1660 nm. These components, although weak, may play a part in the observed dynamics.

4. Conclusions

In this work we report on the observation of a puzzling NLP dynamics in a passively mode-locked fiber laser. Starting from a configuration where conventional, fundamental NLP mode locking is obtained, slight wave retarder adjustments allow entering a regime where the main NLP continually emits sub-pulses that subsequently drift away from the main waveform. Through fine birefringence tuning, different scenarios are successively observed: first, the sub-pulses decay as they move away from the main bunch and then suddenly vanish after a

#242371 Received 4 Jun 2015; revised 6 Jul 2015; accepted 7 Jul 2015; published 13 Jul 2015

fraction of the period; as this time interval is progressively increased, eventually the sub-pulses manage to maintain their amplitude and, after drifting over a complete round-trip time, they are recaptured by the main waveform. Time-domain measurements reveal that the main NLP is actually an aggregate of discrete units at sub-ns scale, with roughly constant energy. These units constitute an intermediate level of organization in the structure of the NLP, and are the elements that are released and drift away from the main packet, either individually or in pairs. The mechanisms underlying the peculiar dynamics reported here and the nearly quantized nature of the intermediate units remain unclear, and will stimulate further research efforts. This work demonstrates once more that passively mode-locked fiber lasers constitute an ideal platform for the study of complex nonlinear dynamics.

Acknowledgments

This work was supported by CONACyT grant 130966. and by CIO-UG 2015 project entitled "*Estudio numérico y experimental de la generación de espectros con ancho de banda amplio en fibras ópticas, para aplicaciones de sensado,*".

#242371 Received 4 Jun 2015; revised 6 Jul 2015; accepted 7 Jul 2015; published 13 Jul 2015